

Review

# Review on Surface Treatment for Implant Infection via Gentamicin and Antibiotic Releasing Coatings

Abhishek Tiwari <sup>1,\*</sup>, Prince Sharma <sup>1</sup>, Bhagyashree Vishwamitra <sup>2</sup> and Gaurav Singh <sup>3</sup>

<sup>1</sup> Department of Metallurgical and Materials Engineering, Indian Institute of Technology, Kharagpur 721302, West Bengal, India; princesharma@alumni.iith.ac.in

<sup>2</sup> Sumiran Women's Hospital & IVF Center, Ahmedabad 380009, Gujarat, India; noddyyishwamitra@gmail.com

<sup>3</sup> Department of Engineering Design, Indian Institute of Technology Madras, Chennai 600036, Tamil Nadu, India; pankaj.gaurav.singh@gmail.com

\* Correspondence: abhishektiwari@iitr@gmail.com

**Abstract:** Surface treatment of metallic implants plays a crucial role in orthopedics and orthodontics. Metallic implants produce side-effects such as physical, chemical/electro-chemical irritations, oligodynamic/catalytic and carcinogenic effects. These effects cause bacterial infections and account for huge medical expenses. Treatment for these infections comprises repeated radical debridement, replacement of the implant device and intravenous or oral injection antibiotics. Infection is due to the presence of bacteria in the patient or the surrounding environment. The antibiotic-based medication prevents prophylaxis against bacterial colonization, which is an emphatic method that may otherwise be catastrophic to a patient. Therefore, preventive measures are essential. A coating process was developed with its drug infusion and effect opposing biofilms. Modification in the medical implant surface reduces the adhesion of bacterial and biofilms, the reason behind bacterial attachment. Other polymer-based and nanoparticle-based carriers are used to resolve implant infections. Therefore, using an implant coating is a better approach to prevent infection due to biofilm.

**Keywords:** gentamicin; infection; biofilm; coating; antibiotic; surface modifications



**Citation:** Tiwari, A.; Sharma, P.; Vishwamitra, B.; Singh, G. Review on Surface Treatment for Implant Infection via Gentamicin and Antibiotic Releasing Coatings. *Coatings* **2021**, *11*, 1006. <https://doi.org/10.3390/coatings11081006>

Academic Editor: Anuj Kumar

Received: 3 August 2021

Accepted: 17 August 2021

Published: 23 August 2021

**Publisher's Note:** MDPI stays neutral with regard to jurisdictional claims in published maps and institutional affiliations.



**Copyright:** © 2021 by the authors. Licensee MDPI, Basel, Switzerland. This article is an open access article distributed under the terms and conditions of the Creative Commons Attribution (CC BY) license (<https://creativecommons.org/licenses/by/4.0/>).

## 1. Introduction

Bone is a structural unit of the skeletal system of vertebrates [1]. Bones are sometimes vulnerable to impacts. Origination of a fracture can be due to several reasons such as, accidents, falling or direct strikes to the body, deficiency of certain nutrients, chronic bone and skeletal diseases, or from injuries while performing day-to-day activities [2]. In human beings, bone ensures the safety of crucial organs such as the heart, lungs and brain [3,4]. Hence, a fracture must be dealt with with utmost priority, and it becomes necessary to heal that fracture, whether it is an open or closed type of fracture. When the magnitude of the fracture is large, metallic implants provide artificial support to the bone. Screws, bone plates, rods, nails and other compression plates are different types of metallic implants used to accomplish bone rigidity [5]. Figure 1 shows a typical virgin metal implant surface, such surfaces are treated as a foreign entity in the human body and soon a defense mechanism is activated. Active inflammation is immediately caused after implantation due to release of cytokines and chemokines from damaged cells [6]. Prolonged active inflammation turns into chronic inflammation which is an indication of infection, side-effect or implant toxicity. Crincoli et al. studied the vitamin D, serum calcium, ionized calcium, phosphorus and Bone Alkaline Phosphatase (BALP) levels in patients with third mandibular molar impaction (TMI) and showed that mandibular third molar impaction could be considered a predictive sign of vitamin D deficiency [7]. Vitamin D plays a major role in craniofacial development and in keeping good oral health [8].

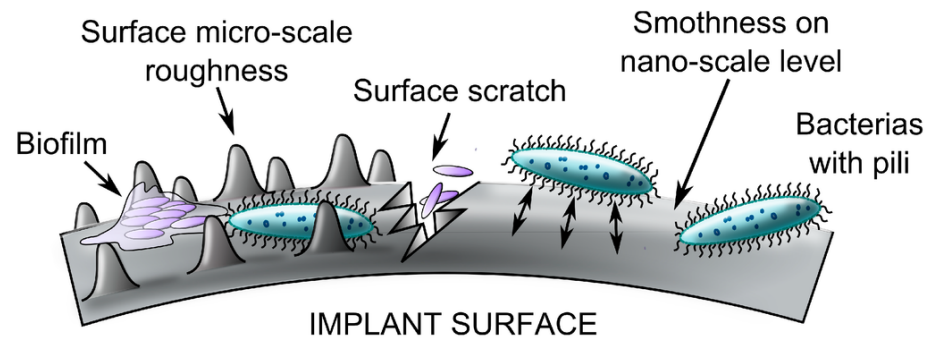


**Figure 1.** Interaction between biomaterial surface roughness and bacterial attachment [9]. Adapted with permission from ref. [9]. A 2014 Creative Commons Attribution (CC BY) license.

Despite much advancement in medicine (antibiotics) and operative treatments, infected non-unions remain a complicated issue [10]. The body treats an implant as a foreign entity and starts to react, causing fever and other medical conditions. The contamination occurred during or after surgery by microorganisms causes infection by adhering to the implant surface. These infections formed over the surface are known as biofilms. These biofilms are formed by complex groups of microbial cells of both Gram-positive and Gram-negative bacteria, forming an extracellular polysaccharide (EPS) matrix. EPS is secreted by bacterial cells, which is an insoluble, organic polymeric substance and slimy in nature. There are five main stages involved in biofilm formation: bacterial attachment to a surface, EPS production, microcolony formation, biofilm formation and detachment of bacteria. Bacterial biofilm involves three layers, making the removal of biofilm difficult from the implant. These layers are named conditioning film, base film, and surface film. Polarity, Van der Waals forces and hydrophobic interaction involve various factors during initial adhesion [11]. Figure 2 shows various types of surgical site infections. If the infection occurs in subcutaneous tissues, it is called a deep wound infection, and if it occurs in soft tissues, it is called an osteomyelitis.

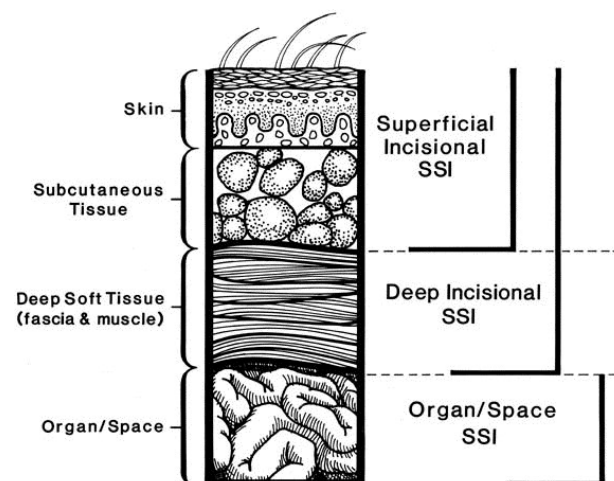


**Figure 2.** Types of surgical site infection (SSI) according to the type of tissue involved [12]. Reprinted with permission from ref [12]. © 1992 Elsevier.

Implant removal followed by re-implantation of the implant are two stages of infection treatment. Infectious biofilms contaminate medical implants and devices, posing serious health risks to patients. Biofilm-associated infection in medical devices is a severe public health concern that also has an impact on the implant's functionality. Surface modification of the device or coating of antibiotics on the implant's surface to kill the microorganisms causing infection prevents infections affiliated with implants.

Although many antibiotics are available commercially, the concentration of antibiotics required plays a crucial part. However, although antibiotics have the property to kill microorganisms and prevent infection, they lack adhesion to the medical implant. Hence, a polymer is necessary along with an antibiotic for binding of the antibiotic onto the medical implant as shown in Figure 3. The polymer must bear properties such as being biodegradable, have good adhesion to the implant surface and must not affect the body's healthy cells [13]. A mixture of an antibiotic with a polymer acts as a source code of surface modification. An implant surface must meet the design parameters of a self-reacting multifunctional micro-machine that releases antimicrobial or other compounds in response to microbiological signals [9]. As a result, antimicrobial surfaces are classed as “contact killing” and antimicrobial agent eluting surfaces [14]. Meningitis (infection of the membranes which provide protection to the brain and spinal cord) and infections of the blood, abdomen (stomach region), lungs, skin, bones, joints, and urinary system are among the risky illnesses brought about by bacteria which are treated with gentamicin injection. Gentamicin is a broad-spectrum aminoglycoside antibiotic that is best used against aerobic Gram-negative and is utilized in a blend with different antibiotics to treat infections caused by Gram-positive organisms such as *Staphylococcus aureus* and certain types of streptococci [15]. It is one of the most frequently prescribed aminoglycosides due to its spectrum of activity, low cost, and availability [16]. Gentamicin is effective against both Gram-positive and Gram-negative organisms but is particularly useful for the treatment of severe Gram-negative infections including those caused by *Pseudomonas aeruginosa* [16]. There is the added benefit of synergy when gentamicin is co-administered with other antibacterials such as beta-lactams [17]. This synergistic activity is not only important for the treatment of complex infections but can also contribute to dose optimization and reduced adverse effects [15,17,18].

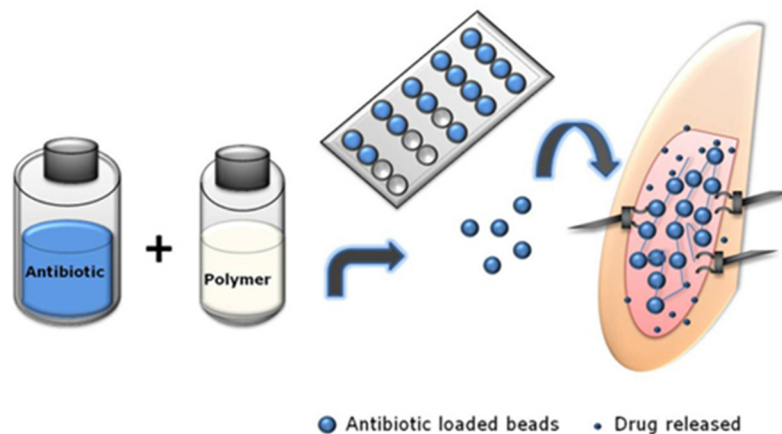


**Figure 3.** The in situ implantation of antibiotic-impregnated beads, as a local antibiotic delivery system, works to obliterate bacteria in the area as well as to reduce the dead space in the bone [19]. Adapted with permission from ref. [19]. A 2013 Creative Commons Attribution (CC BY) license.

Finally, the mixture is mounted to coat on the implant device via various coating processes shown in Figure 4. These different methodologies were used to provide a better assessment of the prophylactic and treatment effects of modified surfaces for biofilm include various approaches for the killing effect, which was assessed via a dip coating, layer by layer, electrodepositing, spray technique [14].

This study evaluates effective surface-modified substances such as antibiotics with a biodegradable adhesive polymer for coating the orthopedic medical implant to prevent and nullify the chances of infection.

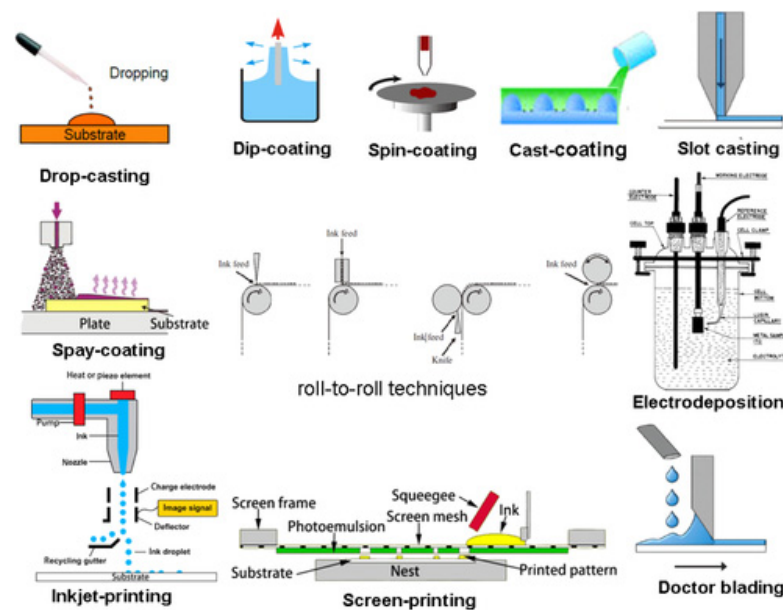


**Figure 4.** Common coating or printing techniques [20]. Reprinted with permission from ref. [20]. © 2017 John Wiley and Sons.

## 2. Pathology of Infection

### 2.1. Etiology of Infection

Osteomyelitis, known as bone infection, is a common issue regarding implants. Infection is a serious dilemma that is difficult to cure without the use of antibiotics. Either antibiotics cure the infection caused by the microorganism, or implant removal is necessary. Infection is in the form of biofilm formation as shown in Figure 5. Osteomyelitis is an infectious disease that causes inflammation of the bone and bone marrow, damaging the bone and necrosis of new bone due to a lack of blood supply [21]. Etiology defines the cause of infection and the possible reasons behind it. Some of the reasons can be: (a) surface of the implant; (b) surgical/operation theatre, surgical equipment and surgeon; (c) from the patient themselves; (d) contaminated disinfectants; and (e) from other persons [22].

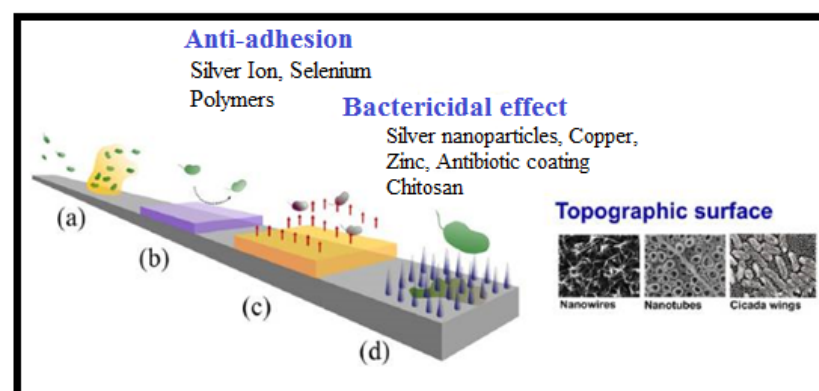


**Figure 5.** Planktonic bacteria forming a biofilm on the material surface: (a) Antibacterial strategies based on ions and polymer coatings ideas of surface chemistry and functionality were employed in a variety of ways; including (b) the surface of the material, which can be coated with bactericidal chemicals such as antibiotics and silver (c) Surface nanopotographic alterations utilized as anti-adhesives or bactericidal agents. (d) Nanotopography examples, such as nanowires, nanotubes, and cicada wings [23]. Adapted with permission from ref. [23]. A 2018 Creative Commons Attribution (CC BY) license.

## 2.2. Microorganism

Microorganisms (not visible with the naked eye) cause infection during surgery or postoperatively from the wound, and postoperative infections mostly restrict the use of implants [24]. In addition, orthopedic infections, including open fractures, are usually caused by Gram-positive and Gram-negative organisms and also by commonly found anaerobes [25]. Therefore, the microorganism causing the infection can be Gram-positive bacteria or Gram-negative bacteria as shown in Figure 6.

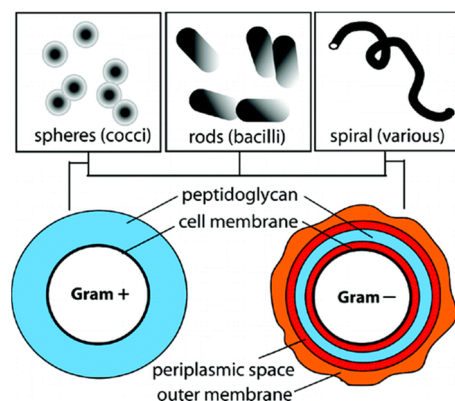


**Figure 6.** Bacteria are classified by shape and then by the outermost cell envelope composition as designated by a Gram-stain [26]. Reprinted with permission from ref. [26]. © 2009 American Chemical Society.

These bacteria are differentiated based on the Gram staining. For example, if bacteria absorb the crystal violet stain and appear to be purple-colored when seen under the microscope, they are Gram-positive. If bacteria do not retain violet color when washed with alcohol after staining and appear reddish or pink when seen under the microscope, they are Gram-negative. The schematic of bacterial attachment is shown in Figure 7. The attachment of bacteria can be through electrostatic, Van der Waals or hydrophobic interactions [27].

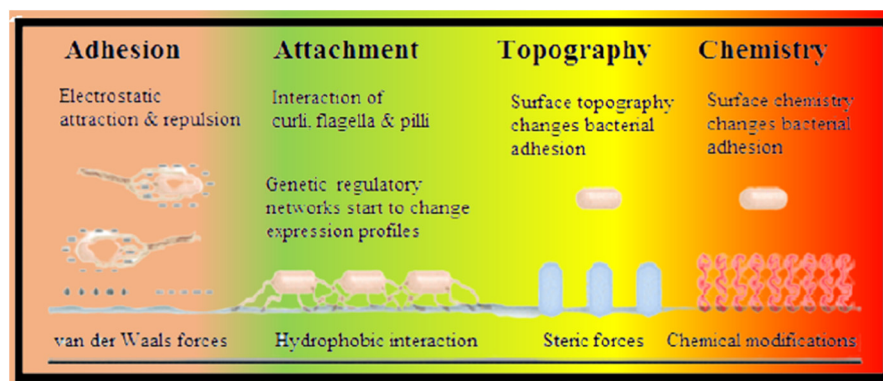


**Figure 7.** Interaction between surface and bacterial cells [28]. Adapted with permission from ref. [28]. A 2013 Creative Commons Attribution (CC BY) license.

## 2.3. Mechanism of Biofilm

A microbial-formed biofilm is an adherent and colony-forming unit of microorganisms within a polymeric substance, typically comprising exopolysaccharides that develop into a complex and wide community [29]. This film is a biologically active form of microbial cells attached to the surface of the implant. The structure formed on the surface could be dynamic and may include single or multiple microbial species [30]. The structure of biofilms is directed by several biological elements such as twitching motility, cell signaling

and responses, growth rate, and EPS synthesis. Biofilm structure may be influenced by the physical development environment. Fluid shear affects a biofilm's physical qualities, including the density and strength, in addition to its structure. The organic polymeric substance EPS (extracellular polysaccharides) is a slimy and insoluble substance secreted by the microorganism on the implant's surface [31]. Polysaccharides, proteins, and nucleic acids make up the extracellular polymeric substance (EPS), which is vital for safeguarding biofilm microorganisms. The interstitial spaces allow easy access to nutrients and oxygen from the bulk fluid and the removal of metabolic wastes. As a result, the attached microbes form colonies on the implant. Hence, biofilm formation takes place. As shown in Figure 8, the biofilm's growth and development is divided into five stages: in the first, cells adhere to the surface and create extracellular polysaccharides (EPS), which leads to biofilm formation. Stage 2 is the production of EPS followed by stage 3, the early development of the biofilm, and finally stages 4 and 5 are the maturation of the biofilm and dispersion of cells from the biofilm, respectively. Due to the unfavorable environmental conditions, the matured bacterial colony becomes isolated as shown in Figure 9 and begins to circulate in a single-cell form. The dispersed cells spread away and adhere to the favorable surface matrix [32]. The biofilm layers constitute three layers: (a) the initial layer or conditioning film, bonded to the implant material; (b) the biofilm base, which consists of microbe; and (c) the outer layer or surface film where free-floating organisms are released and then spread to the surroundings [13,33–35].

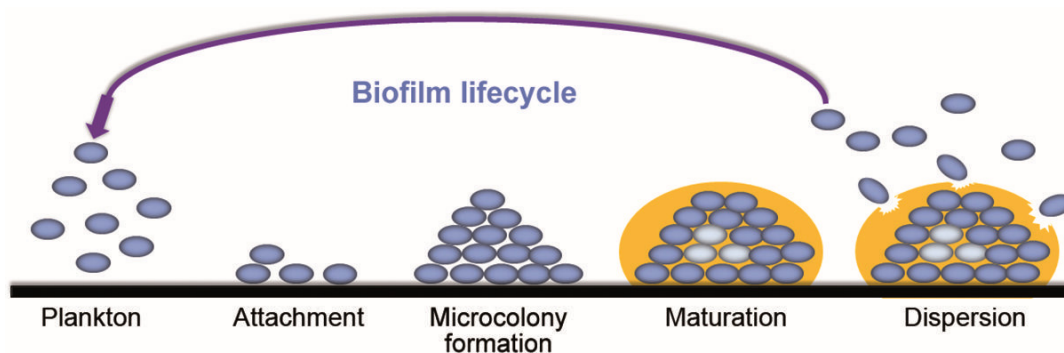


**Figure 8.** Biofilm development steps produced by microorganisms [36]. Adapted with permission from ref. [36]. A 2018 Creative Commons Attribution (CC BY) license.

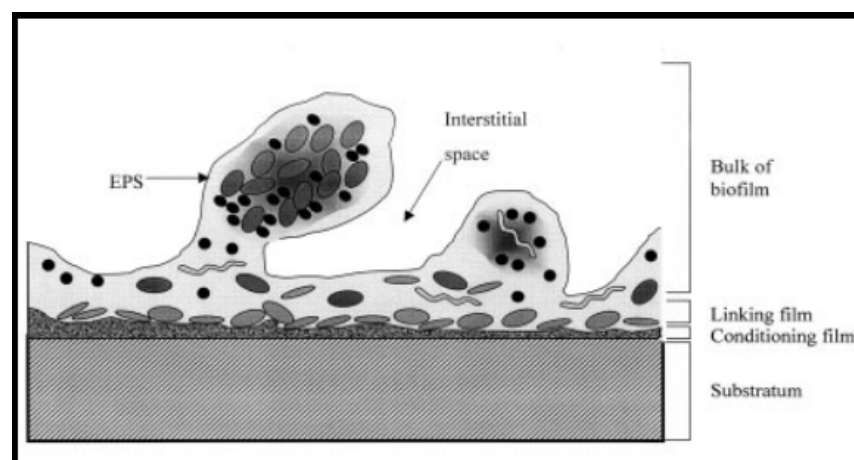


**Figure 9.** Mature biofilm layers, including the bulk of the biofilm, linking film, conditioning film, and the substratum to which the film is attached [37]. Reprinted with permission from ref. [37]. © 1999 John Wiley and Sons.

### 3. Antibiotics and Antibiotic Imitated Coatings

One of the major causes for the reason of death is health-associated infections. There are several medical device health-associated infections (MDHAI) varying from high infection rates to low infection rates. These incidences may depend on the number of factors linked, which include the type of medical device, their anatomical location or the usage of the treating antibiotic, morbidity, mortality, the microorganism involved, and therapeutic treatments. To avoid MDHAIs, the use of antimicrobial and anti-biofilm strategies is common. The role of the biofilm is crucial to understand MDHAIs [38,39]. The antimicrobial or antibiotic coating is one of the widely used medical device technologies to prevent biofilm formation. Anti-adhesive coatings are intended to prevent the first stage of biofilm formation, colonization, and so eradicate the problem from the start. A microorganism that adheres to surface specifically or non-specifically interacts, absorbing biological molecules forming a bacterial adhesion and biofouling [40]. Various anti-adhesive coatings, such as polyethylene oxide (PEO) and zwitterionic polymers, are coatings designed to prevent biofouling [41,42]. In addition, the fabrication of coatings with nanoparticles/microparticles was amended to deter microbial sticking [43,44]. The influence of biofouling on the performance of a coating is a significant constraint for all forms of anti-adhesive coatings. The most commonly used coatings are coatings that are loaded with antimicrobial agents. Polymer and hydrogel coatings contain a wide range of antimicrobials [45]. Depending on the application, the coating material is adjusted to secrete various antimicrobials at different scales. Thus, to respond to parameters such as temperature, pH, or other changes produced by the presence of microbes, the development of advanced controlled-release coatings is essential [46–48]. Most of the antimicrobial agents in medical devices are drug composite products that have been legally marketed, for instance, antibiotics and metal ions. Gentamicin, tobramycin, rifampicin, and clindamycin are among the antibiotics utilized in medical devices [49]. Figure 10 shows a smoother coating of Poly-d,l-lactic acid (PDLLA) compared to Titanium [50]. It was found that biodegradable PDLLA coatings released bioactive substances for over 42 days [51]. The coating of implants enables them to function as carriers for biological substances and provide mechanical stabilization. Antibacterial coatings have been classified in the following ways of modification according to their mechanism of operation. Examples include polymer coatings. Surface or structure modification as passive surface finishing aimed at preventing or reducing bacterial adherence to implants, with the exclusion of any pharmacologically integrated chemicals. Examples include polymer coatings. Surface modification occurs when pharmacologically active compounds such as antibiotics, antiseptics, metal ions, or other compounds are vigorously freed from the surface to inhibit bacterial adhesion [52]. These may even include pre-incorporated bactericidal agents to reduce the adhesion. Examples include silver- or iodine-coated implants as shown in Figure 11. Silver and iodine are known for antibacterial and antiseptic properties, respectively. Local antibacterial carriers or coatings are used in preoperative antibacterial carriers or coatings, which are not integrated into the device but are placed during surgery just before the implant is inserted. They may have a direct antibacterial/anti-adhesive function or provide a high concentration of loaded antibiotics [53].

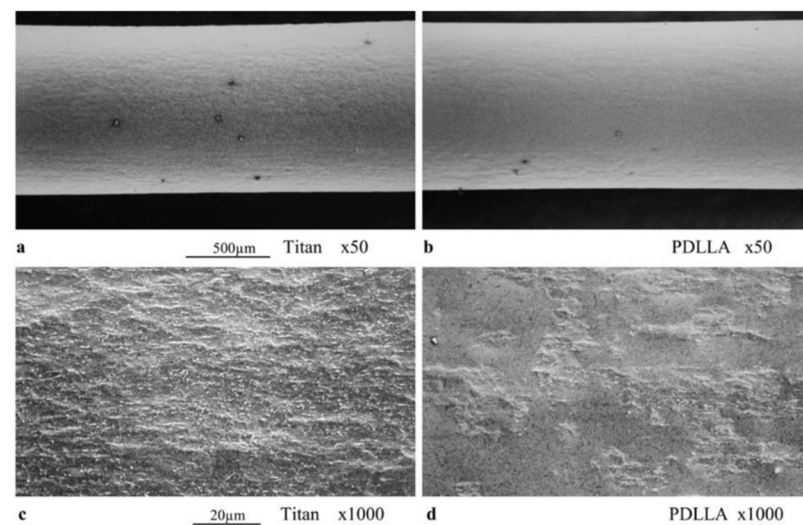


**Figure 10.** Comparing electron microscopic images of Titanium implants (surface modification) (a) without PDLLA at 50 $\times$ , (b) with PDLLA at 50 $\times$ , (c) without PDLLA at 1000 $\times$ , and (d) with PDLLA at 1000 $\times$  [50]. Reprinted with permission from ref. [50]. © 2006 Springer Nature.



**Figure 11.** Examples of antibacterial coatings: (A) silver-coated; (B) iodine-coated; (C) vancomycin-loaded Defensive Antibacterial Coating (DAC) hydrogel, applied at the time of surgery on an acetabular titanium component [54]. A 2019 Creative Commons Attribution (CC BY) license.

#### 4. Mechanical Properties and Characterization of Gentamicin and Its Composites

Strobel et al. tested the mechanical axial rigidity of gentamicin-coated wires via standard bending test [55]. They recorded no elongation on the site of application of pressure while an approximate elongation of 1.5% was recorded on the fixed side. The mechanical properties of the acrylic bone cement used in orthopedic surgery play a key role in determining a prosthesis's long-term stability [56]. The chitosan (CS) powder can easily be mixed with PMMA bone cement powder and cast [56]. When the CS/bone cement powder weight ratio is 30%, Young's modulus is drastically lowered (Figure 12) [56]. Even when the CS loading is lowered to 15%, the Young's and bending modulus are roughly 90% of the original bone cement's comparable properties. When the chitosan was added in the form of nanoparticles instead of powder, the bone cement can better retain its mechanical properties [56]. For example, the addition of chitosan nanoparticles up to a chitosan/bone cement powder ratio of 15% does not result in a significant loss of Young's and bending modulus (Figure 12) [56]. When nano-sized CS is employed, the composite cement's mechanical properties improve due to its more uniform dispersion in the PMMA matrix, resulting in no "macroscopic" weak links in the cement. Figure 12 shows the Young's and bending modulus of the original and modified bone cement decrease by ~10% or less after 3 weeks immersion in phosphate-buffered saline (PBS) (pH = 7.4) [56]. The maximum reduction in Young's modulus was observed for the cement loaded with CS powder at weight ratios of 15% and 30% [56]. There are no significant difference in

mechanical properties of the quaternary ammonium chitosan derivative nanoparticles (QCS NP) loaded cement and chitosan nanoparticles (CS NP) loaded cement, either in the freshly prepared form or after extended immersion in PBS [56]. The mechanical tests on the various gentamicin-loaded types of cement before and after 3 weeks in PBS also produce similar results [56]. These observations show that antibacterial assays were carried out with composites with a CS or QCS to bone cement powder weight ratio of 15% in order to achieve a balance between mechanical strength and antibacterial effectiveness [56].

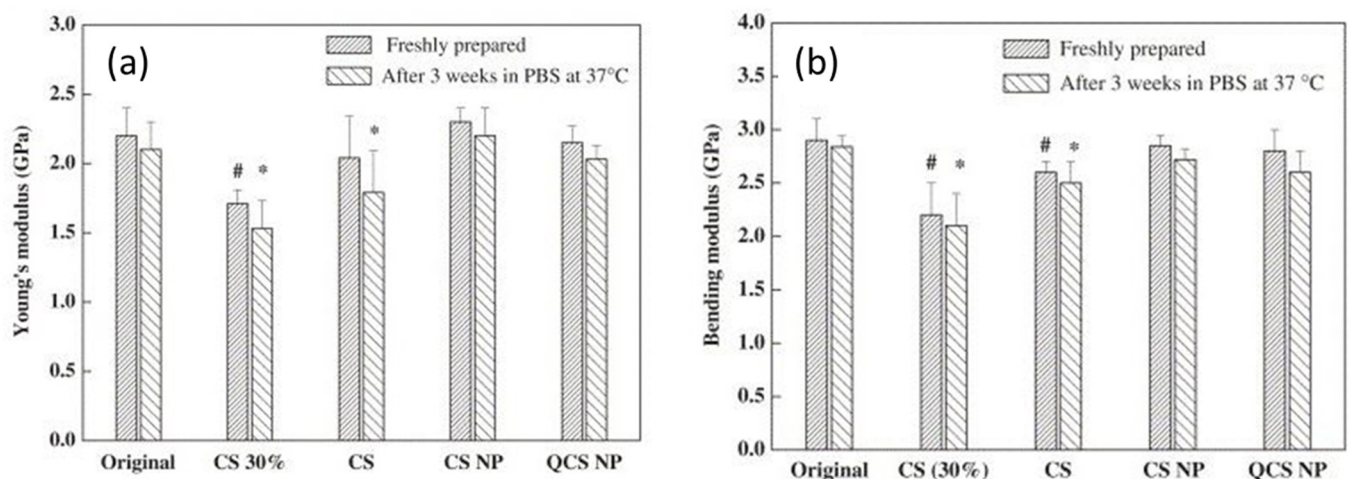


**Figure 12.** (a) Young's modulus of original and C.S. (30%), C.S., CS NP- and QCS NP-loaded Smartset plain and gentamicin-loaded. (b) Bending modulus of original and C.S. (30%), C.S., CS NP- and QCS NP-loaded Smartset plain and gentamicin loaded. Except for C.S. (30%), the other substrates were mixed at a weight ratio of C.S. or QCS to PMMA bone cement powder of 15%. (#), (\*) denote significant differences ( $p < 0.05$ ) compared with original bone cement, which is freshly prepared or after three weeks in PBS [56]. Reprinted with permission from ref. [56]. © 2006 Elsevier.

A linear elasticity zone ending at the yield strength, followed by a protracted plateau displaying sustained flow stress to tremendous strain, characterizes porous materials under compressive load. The different parameters such as number, size, shape and connectivity of pores affect Young's modulus and yield stress. Cancellous bone has a porous structure, and the porosity of cancellous bone impacts the resulting mechanical properties—cancellous bone yield stresses range from 3 to 20 MPa, with corresponding Young's moduli ranging from 10 to 40 GPa [57]. Therefore, the pore formation can support the material by satisfying the natural bone system (elastic modulus ranging from 3 to 20 GPa, Table 1) and also by increasing biological integration [57].

**Table 1.** Physical and mechanical properties of various implant materials in comparison to natural bone [57].

Properties	Natural Bone	Magnesium (Mg)	Ti Alloy	Co-Cr Alloy	Stainless Steel (SS)
Density ( $\text{g}/\text{cm}^3$ )	1.8–2.1	1.74–2.0	4.4–4.5	8.3–9.2	7.9–8.1
Fracture toughness ( $\text{MPa}\cdot\text{m}^{1/2}$ )	3–6	15–40	55–115	N/A	50–200
Elastic modulus (GPa)	3–20	41–45	110–117	230	189–205
Compressive yield strength (MPa)	130–180	65–100	758–1117	450–1000	170–310

The primary issue with implant materials is their high Young's modulus for metallic-based materials and low mechanical characteristics for very porous polyester-based ma-

materials. These issues can be resolved by providing adequate porosity to these metallic materials. For example, Ti metallic foams have 78% porosity, whereas Mg foams have 50% and the strength 35 and 2.33 MPa respectively, while the strength of bone is in the 3–20 MPa range [58]. Furthermore, Young's modulus of Ti and Mg foams are 5.3 and 0.35 GPa, respectively, which are closer to Young's modulus of bone [58,59].

Qualitative and quantitative analysis of a sample involves spectroscopic methods based on emission, absorption, fluorescence, or scattering phenomena. Raman spectroscopy is a scattering technique that works on the principle of the Raman effect, which states that the frequency of a small proportion of scattered radiation differs from the frequency of monochromatic incident light. The inelastic scattering of incident light as it interacts with vibrating molecules is the underlying mechanism [60,61]. Raman spectroscopy provides extensive information on analytic identification, sample matrix characterization, and molecular spectroscopic information that can be utilized to analyze structural entities [62]. It is a rapid procedure, and when combined with methods of sample preparation, for instance, micro-extraction, fraction collections and analysis of small particles, a single piece of forensic evidence provides a large amount of information [63]. Raman spectroscopy is currently commonly utilized to determine drug/polymer composition, drug distribution within the polymer matrix, drug coating thickness, and drug release kinetics [64]. Figure 13a shows the polymer/drug bilayer in the stem section [64]. For gentamicin, the band near  $1500\text{ cm}^{-1}$  is the typical N-H stretching vibration (Figure 13b) [64]. The Raman spectra of the Poly(lactic-co-glycolic acid) (PLGA) and gentamicin sulfate (GS) bilayer at various Z heights from the surface (0) to  $12\text{ }\mu\text{m}$  inside the sample are shown in Figure 13 [64]. The peaks for the GS can be seen at  $980$  and  $1500\text{ cm}^{-1}$  due to the asymmetric stretching vibration of  $\text{SO}_4^{2-}$  and the stretching vibration of N-H, respectively [64]. The PLGA is determined by characteristic ester group peak at  $1770\text{ cm}^{-1}$  and the asymmetrical stretching of the C-O-C band at  $1046\text{ cm}^{-1}$  [64]. The peak height increases as the laser penetrates deeper into the sample and lowers as the laser moves away from the material's center. By studying such Raman spectra, the thickness of PLGA may be estimated [64].

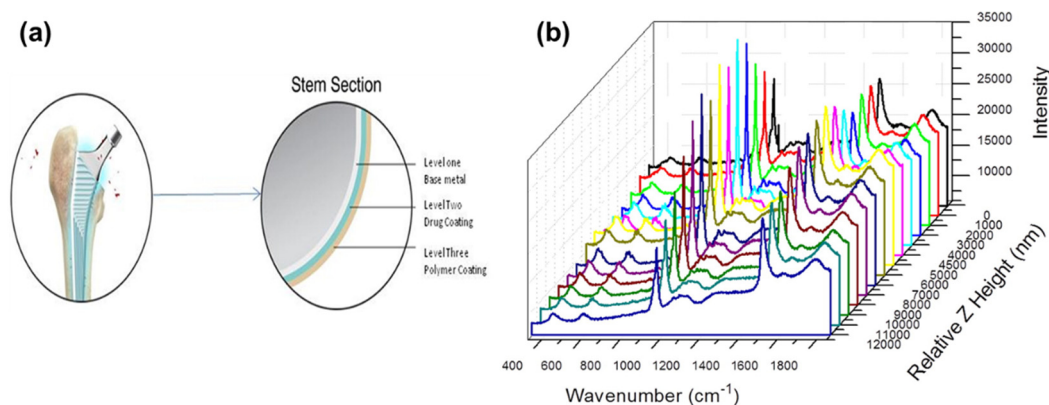


**Figure 13.** (a) Schematic diagram of the stem section showing the polymer/drug bilayer, (b) plots of GS and PLGA Raman spectra from the confocal Raman spectrum as the laser moves through the Z height [64]. Reprinted with permission from ref. [64]. © 2013 American Chemical Society.

The ester group bands at  $1770\text{ cm}^{-1}$  represent PLGA, while the C-O-C band's asymmetrical stretching at  $1046\text{ cm}^{-1}$ . According to this graph, the peak height rises as the laser penetrates further into the sample and decreases as the laser advances away from the material's center. These spectra are used to determine the thickness of PLGA. Each spectrum's peak area was measured at  $980$  and  $1770\text{ cm}^{-1}$  for GS and PLGA, respectively (Figure 13b). Another finding from the spectra is that these bands have no Raman shift, showing that the PLGA and GS are not mixed together [65].

Nast et al. found the C-H bonds at approximately  $2995$  and  $2946\text{ cm}^{-1}$  and the C-O bond nearly at  $1746\text{ cm}^{-1}$ , indicating a minor change in the bond energy of PDLLA [66].

However, I.R. bands could not be easily detected in the coating spectrum because of the excess presence of PDLLA in the antibiotic [66]. Nevertheless, in a magnified view of characteristic I.R. bands of gentamicin sulfate approximately at 1614 and 1524  $\text{cm}^{-1}$ , the lower spectrum could be recovered in the middle spectrum of PDLLA and gentamicin sulfate coating resulting in no change in the nature of the antibiotic [66].

In Figure 14, Li et al. observed the distinctive peaks for Gelatin, the amide group types I (1645  $\text{cm}^{-1}$ ), the amide group types II (1542  $\text{cm}^{-1}$ ), and the amide group type III (1238  $\text{cm}^{-1}$ ) [67]. The strong characteristic peaks for GS were the strong and medium absorption peaks for  $\text{SO}_4^{2-}$  were observed at 1124  $\text{cm}^{-1}$  and 618  $\text{cm}^{-1}$  respectively [67]. The GS-loaded Ti-G composite exhibited two peaks at 1107  $\text{cm}^{-1}$  and 618  $\text{cm}^{-1}$ , distinctive peaks of the  $\text{SO}_4^{2-}$  in the GS [67].

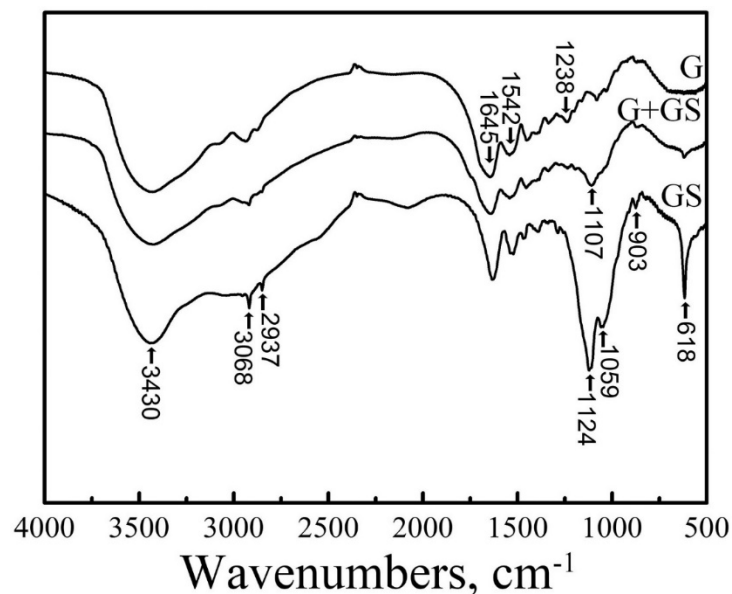


**Figure 14.** FTIR analysis results of the gelatin, GS and GS-loaded gelatin [67]. Reprinted with permission from ref. [67]. Reprinted with permission from ref. [67]. © 2016 Elsevier.

The spectral graph for  $\text{CaCO}_3$  nanoparticles (CCNPs) show peak absorption at 875 and 713  $\text{cm}^{-1}$ ,  $\text{CO}_3^{2-}$  bending vibration of calcite polymorph are recognized at bands at 876  $\text{cm}^{-1}$ , the band around 3448  $\text{cm}^{-1}$  in gentamicin sulfate (GS)-loaded CCNPs (CGPs) was confirmed as the  $-\text{OH}$  stretching vibration of the captivated water. The spectrum of GS, exhibited the bands at 1631 and 1535  $\text{cm}^{-1}$  (N–H bands), 1130  $\text{cm}^{-1}$  (C–O bands) (Figure 15) [68]. The spectra of gentamicin sulfate (GS)-loaded CCNPs [CGPs] revealed the most characteristic bands for both gentamicin sulfate (GS) and CCNPs, showing that the drug was effectively loaded onto CCNPs. After juxtaposing the spectra, the new band appeared at 1421  $\text{cm}^{-1}$  and bands at 1631 and 1535  $\text{cm}^{-1}$  escaped. As a result, we hypothesized that an H-bonding contact could exist between the medicine and the carrier (as shown in Figure 16).

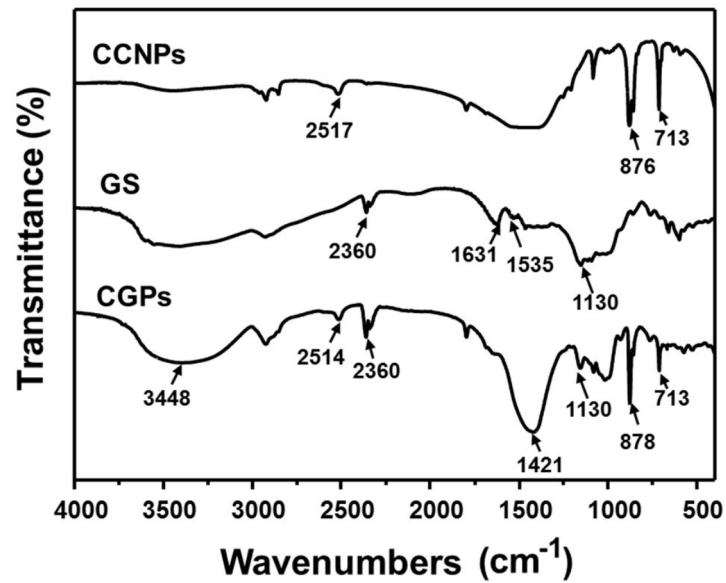


Figure 15. FTIR spectra of CCNPs, GS, and CGPs [68]. Adapted with permission from ref. [68]. A 2018 Creative Commons Attribution (CC BY) license.

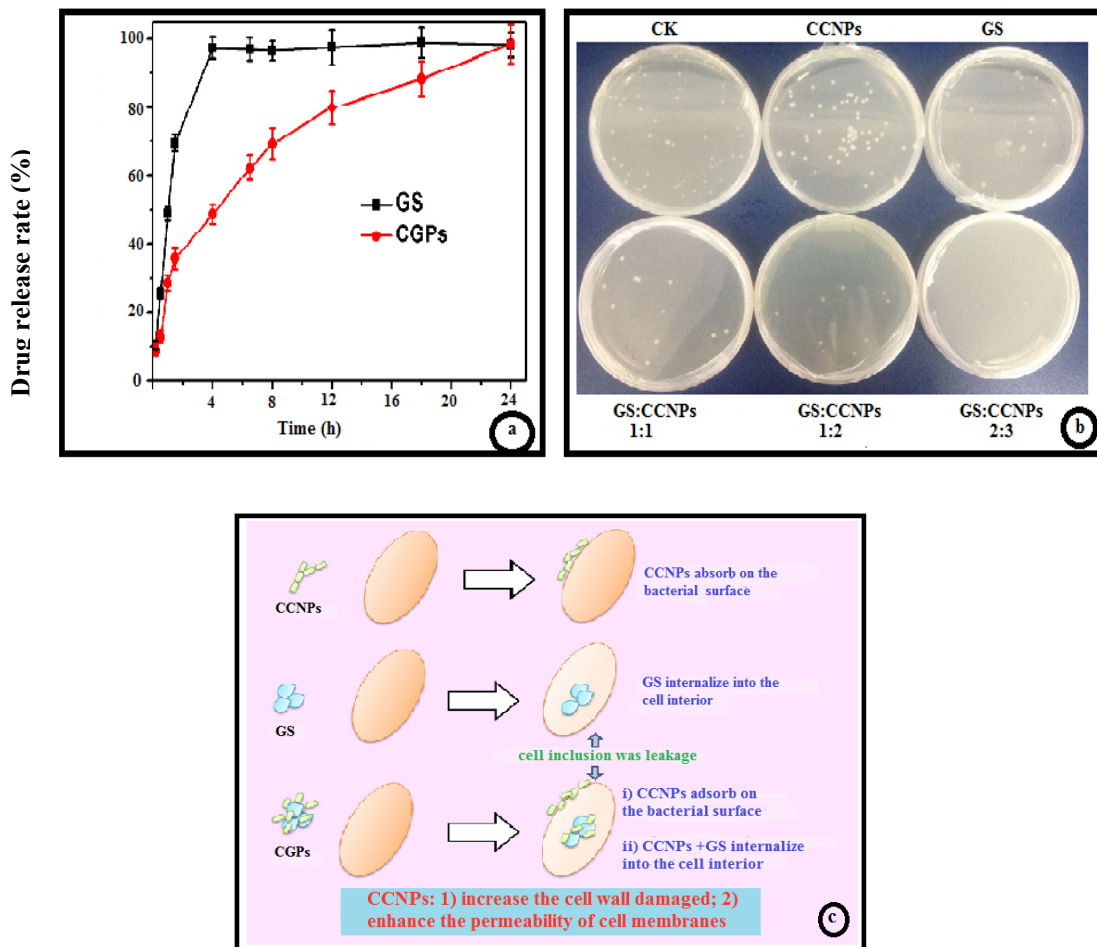
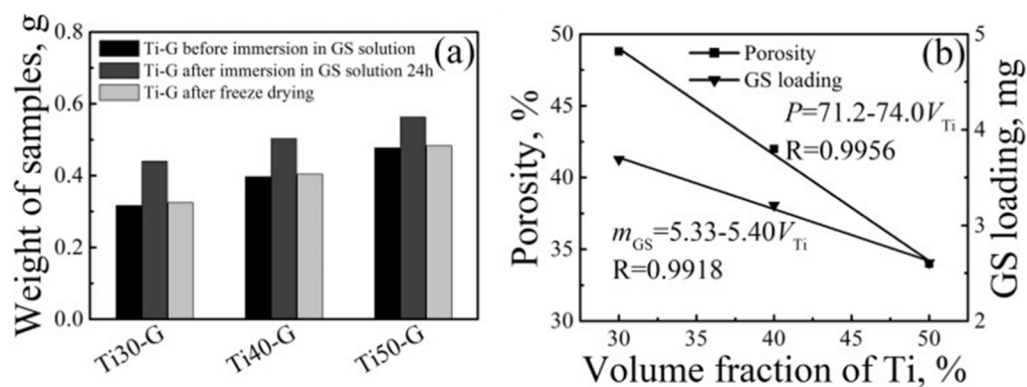


Figure 16. (a) The in vitro release profiles of the drug (GS concentration). (b) The colonies of *B. subtilis* treated by CCNPs, GS, and CGPs. (c) Schematic representation of the synergistic antibacterial mechanism between nanoparticles aggregates and drugs [68]. Adapted with permission from ref. [68]. A 2018 Creative Commons Attribution (CC BY) license.

The drug release under controlled conditions was assessed by dissolution tests. Figure 16a shows the release rate of pure gentamicin sulfate and CaCO<sub>3</sub> gentamicin nanoparticles. It was observed that 50% GS was released from pure GS within one hour, but 50% GS was released from CGPs after four hours. Meanwhile, the pure GS medication was totally released within four hours, whereas GS from CGPs was totally released for up to 24 h. As a result, GS release from CGPs was slower than pure GS. On an agar plate, the bactericidal activity of GS, CCNPs, and CGPs was determined by Pan et al. [68]. According to the statistics, the antibacterial action of CCNPs was insufficient (12.43 percent), but the GS displayed minor antibacterial activity against B [68]. The inhibition rate of subtilis was 22.84%. GS, on the other hand, exhibits a strong inhibition rate of 69.79 percent following loading onto CCNPs. Thus, the finding indicated that successful integration of GS into the core of CCNPs, and integrated GS could increase the antibacterial activity taken together to CCNPs. Thus, resulting in the maintenance of its biological activity, the antibacterial activity was greatly enhanced. Furthermore, the solid agar plate method confirmed that CGPs had much higher antibacterial efficacy (Figure 16b). Antibacterial activity responded in such a pattern as: GS: CCNPs = 2:3 > GS: CCNPs = 1:2 ≈ GS: CCNPs = 1:1 > GS > CCNPs.

Pan et al. proposed the probable CGPs antibacterial mechanism (Figure 16c) [68]. First, the bacterial surface possibly absorbs CCNPs due to intermolecular forces (with a negative charge and small size). As a result, CGPs had a higher likelihood of interacting with bacterial surfaces. Second, as CCNP carriers cause more damage, the cell wall and GS increase the permeability of cell membranes, resulting in internalization into the cell interior and the death of bacteria.

Characterization of the GS-loaded Ti-G composites, the author Li et al. demonstrated that Gelatin is a good absorbent in GS solution, drug-loading can be accomplished simply by immersing the samples in GS solution, and the amount of the GS-loaded can be calculated simply by weighing the samples, as shown in Figure 17a [67].



**Figure 17.** (a) Weights of the Ti-G samples before and after immersion in GS solution 24 h, and weights after lyophilization; (b) the amounts of the loaded GS and the porosities of GS-loaded Ti-G composites [67]. Reprinted with permission from ref. [67]. © 2016 Elsevier.

Considering the size of samples to be  $5 \times 10 \text{ mm}^2$ , the quantity of the GS-loaded was 3.65 mg, 3.21 mg, 2.61 mg for Ti30-G, Ti40-G and Ti50-G, respectively. The porosity of samples Ti30-G, Ti40-G and Ti50-G came out to be 48.8%, 42.0% and 34.1%, respectively. With such data, two linear correlations could be tentatively constructed between actual porosity ( $P$ ) and volume fraction ( $V_{Ti}$ ), or between the amounts of GS-loaded ( $m_{GS}$ ) and volume fraction ( $V_{Ti}$ ) (as shown in Figure 17b). Gelatin being degradable inside the human body would gradually create free spaces after implantation, indicating that the larger the porosity, the more bone cell ingrowth and prosthesis fixation [67].

## 5. Microbial Assay

The antibacterial activity in vitro tests were performed by observing that the nails containing gentamicin maintained for at least 12 days showed a strong antibacterial activ-

ity [69]. Furthermore, PLA + CF + Alg + GS showed higher inhibition zone growth than PLA + Mg + GS (Figure 18).

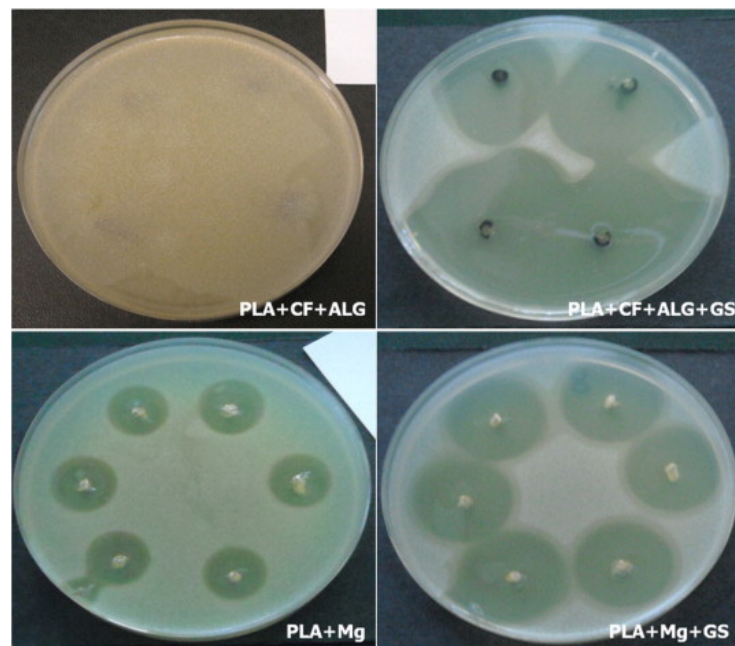


**Figure 18.** Inhibiting effect of the nails with a gentamicin addition by the growth of the methicillin-sensitive *Staphylococcus pseudintermedius* strain (culture after 48 h of incubation) [69]. Reprinted with permission from ref. [69]. © 2014 Elsevier.

Antibiotic gentamicin liberated *in vitro* was the initial blowout. After 1 min, 60% of the assimilated antibiotic was discharged into PBS solution from the coated layer. This active release of antibiotics was continued further by a slow, stable and steady release. An additional antibiotic of 10% and 85% separated from the coating (Figure 19a) after three and six weeks, respectively.

Gentamicin was applied on agar plates with *Bacillus subtilis* and 10  $\mu$ L of each sample from the *in vitro* trials [70]. After plates incubation, the antibacterial efficacy was checked at 37 °C for 10 s, 20 s, 30 s, 60 s, 2 min, 3 min, 4 min, 5 min, 10 min, 30 min, 60 min and 24 h, giving zone of inhibition [70]. On agar discs incubated with *Bacillus subtilis*, all samples show appropriate zones of inhibition. The diameter ranged from 11 mm after 10 s to 17 mm after 24 h (Figure 19b) [70].

Bacterial adhesion on the implant was efficiently achieved after 1 min and 10 min of incubation in an *S. epidermidis* suspension. Vester et al. observed greater Colony Forming Units (CFUs) on the uncoated K-wires compared to PDLLA wire (Figure 19c) [70]. At PDLLA + 10% gentamicin, wires counted the lowest CFU levels.

In Luria–Bertani (L.B.), the antibacterial effectiveness of GS-loaded Ti-G was investigated. Figure 20 depicts the medium. Li et al. reported no bacteria inhibiting loop around the Ti-G sample after 24 h, but a distinct bacteria inhibiting loop around the GS-loaded Ti-G sample [67]. As a result, this GS-loaded Ti-G material appears to be sufficient to prevent bacteria development and minimize the frequency of infections following this biomaterial implant.

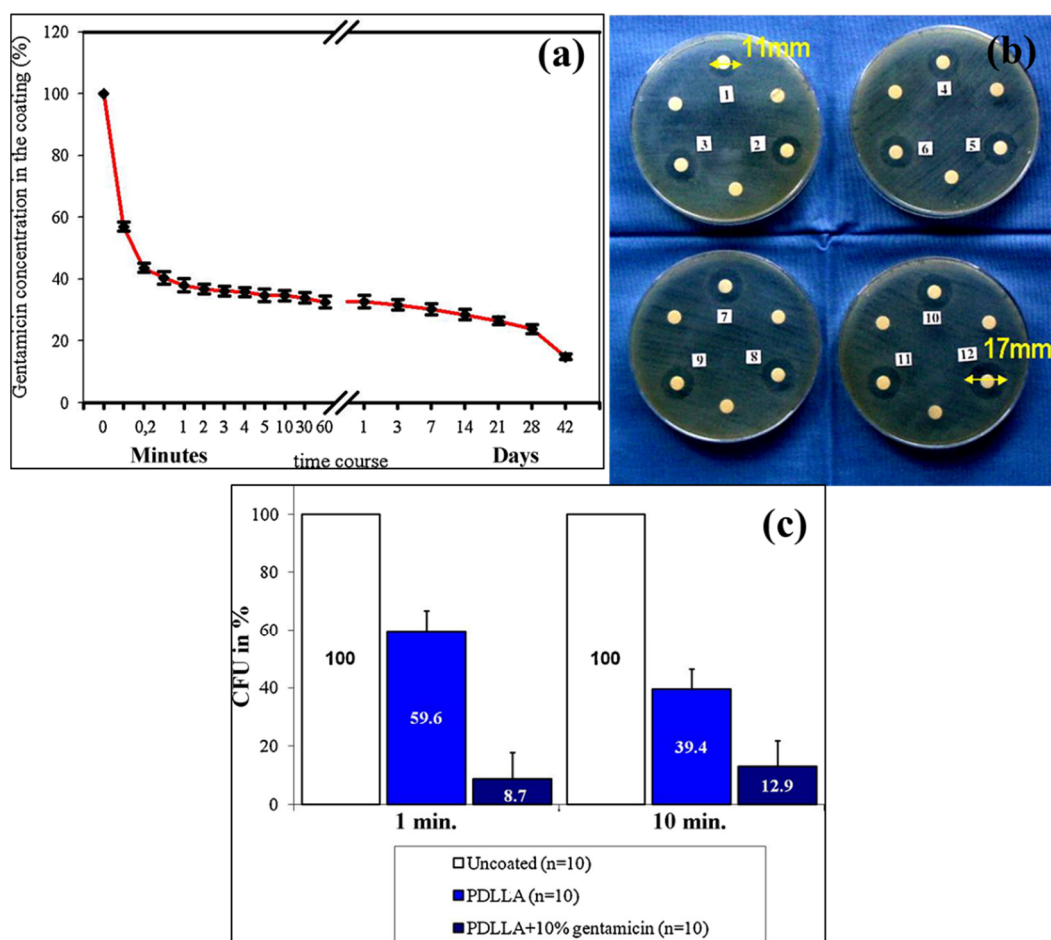


**Figure 19.** (a) Gentamicin release in vitro for 42 days (mean values), (b) depicts the test sites of the agar diffusion test clearly with the zones of inhibition, (c) bacterial adhesion over nutrient agar plates: average CFU after rolling uncoated, PDLLA-coated and PDLLA + 10% gentamicin coated K-wires [70]. Reprinted with permission from [70]. © 2010 Elsevier.



**Figure 20.** Antibacterial test of GS-loaded Ti-G after 24 h [67]. Reprinted with permission from ref. [67]. © 2016 Elsevier.

### 6. Clinical Studies

Though after such hard protection of bone, still, bone gets infections when exposed to some fracture. There is a requirement of antibiotics to treat such infections, and there is a long period of consumption of antibiotics to treat such infections. Bone infections are common health issues that are regarded as a representation of suffering, morbidity, destruction, and death [71]. Local antibiotic therapy is a common method to treat arthroplasty infections,

prophylaxis for fractures, and treatment of chronic osteomyelitis. Treatment can be difficult and time-consuming because it is dependent on antibiotic penetration to the infection site [72]. Antibiotics of various types are available, and every antibiotic works against the microorganisms and inhibits their reproduction and, after that, the blockage of the protein. Until now, antibacterial coatings are employed in several studies for the prevention of contamination. The biodegradable polymer PDLLA [poly (D, L- Lactic acid)] with gentamicin sulfate and other antibiotics is an implant-coating material. Strobel et al. observed that the concentration ratio for a polymer and the amount of drug are important criteria for the release rate of the coating material and the mechanical stability of the polymer at different concentrations [55]. Lakdawala et al. developed a methodology for coating using an aerosol spray technique by composites of biodegradable polymer and drug [13]. The authors observed the gentamicin concentration in polymer and the thickness of the coated film, which controls the release of the drugs [13]. Pan et al. developed an effective way for the delivery of the drug by incorporation of CaCO<sub>3</sub> nanoparticles as drug carriers [68]. Then the authors observed that CCNPs lengthen the release of the drug and increased the antibacterial activity of the drug [68]. Metsemakers et al. used ETN PROtect gentamicin-coated nails to prevent deep infection of the bone [73]. In the study, the authors included patients with a number of injuries and difficult revision cases [73]. Thonse et al. concluded using local antibiotic delivery to control infection by impregnating gentamicin with PMMA avoids the need for second surgery [74]. Morawska-Chochol et al. introduced gentamicin sulfate in the PLA matrix on magnesium or carbon and alginate fiber implants [75]. The local drug therapy enhanced and prolonged the inhibitory effect for microbial growth [69]. Raj et al. concluded gentamicin-loaded antibiotics with ceramic polymer coating was the simplest method to eradicate osteomyelitis and bone defects [76]. Saravanan et al. windup indicate antibiotic cement coating implant provides an easy, prudent and very efficient, effective way for the treatment of non-unions [77]. Schmidmaier et al. observed coating of an implant integrated with an active form of growth factors [51]. The authors observed fracture healing properties due to the coating layer's growth factors and high mechanical stability [51]. He et al. summarized by creating gentamicin sulfate in PAA (Poly Acrylic Acid) multilayers on Ti alloy implants showed excellent antimicrobial effects against S.aureus and E.coli [78]. A summary of the above-mentioned clinical studies is listed in Table 2 shown below.

**Table 2.** Summary of clinical studies.

Authors	Material	Process of Coating	Reference
Lakawala et al.	PMMA, PDLLA, gentamicin	Aerosol spray technique	[13]
Pan et al.	gentamicin, CaCO <sub>3</sub> nanoparticles.	Dip-coating method	[68]
Morawska-chochol et al.	PLA, Mg, Tricalcium phosphate (TCP), GS, Carbon fiber (C.F.), Alginate Fibre (Alg)	Injection molding method, etching method	[69]
Vester et al.	Gentamicin sulphate, PDLLA, Ethyl acetate solution,	Dip-coating	[70]
Metsemakers et al.	Gentamicin coated tibia nail, PDLLA	Dip-coating method	[73]
Thonse et al.	Gentamicin, PMMA	Metal molds	[74]
Raj et al.	Ti sheet, TiO <sub>2</sub> -SiO <sub>2</sub> ceramic, chitosan-lysine (CS-LY-1,2,3) composite, gentamicin	Anodization method, electrodeposition method	[76]
Saravanan et al.	Vancomycin, gentamicin bone cement, K-nail	-	[77]
Schmidmaier et al.	PDLLA, Chloroform, growth factors	Cold coating technique	[51]
He et al.	Gentamicin, Polyacrylic acid (PAA), NaOH solution	Layer by layer	[78]
Bhatia et al.	Bone cement, Vancomycin, Teicoplanin, PLLA (polymer)	Push method through endotracheal tube	[79]
Vicenti et al.	Gentamicin coated I.M. tibia nail (ETN PROtect DePuy Synthes), Reaming irrigation aspiration.	Dip-coating method.	[80]
Pinto et al.	Gentamicin, Poly (D, L-lactide)	Dip-coating process	[81]
Moghaddam et al.	Gentamicin coated ETN, Polylactide acid (PDLLA)	Dip-coating process	[82]
Khodaei et al.	Ti powder, NaCl (as a spacer agent), Gelatin and strontium hydroxide mixture, gentamicin, Poly-vinyl alcohol (PVA).	Deposition method	[83]
Neut et al.	Ti alloy coupon, GS, polylactic glycolic acid, bone cement with polytetrafluoroethylene (PTFE).	Spraying technique	[84]
Raschke et al.	Gentamicin, PLLA Tibia nail (UTN Protect)	Dip-coating method	[85]
Lucke et al.	K-wire, PBS solution, PDLLA, GS, Group I—K wire (uncoated+PBS as control), Group II—K wire without coating, Group III—K wire coated with PDLLA, Group IV—K wire coated with PDLLA + 10% GS	-	[86]
Gollwitzer et al.	PDLLA, ethyl acetate, gentamicin, teicoplanin,	Dip-coating	[87]
McMillan et al.	PDLLA in 3 combinations: 1. gentamicin sulphate(GS), 2. vancomycin sulphate (VS), 3. Gentamicin-palmitate (GP)	Dip-coating	[88]

## 7. Conclusions

Microorganisms are cosmopolitan organisms indicating their presence everywhere. Biofilm formation by them is pervasive and resilient to annihilate. Therefore, the focus must be on infection prevention rather than treatment as “prevention is better than cure”. The device’s outlined stages of bacterial biofilm formation interfere with the surface and cover the implant application and function. Therefore, preparing surfaces free from contamination, antimicrobial and anti-biofilm techniques on the medical device is associated with eradicating the cause. To reduce infection rates, many techniques were developed for improvement as bacterial infections are very frequent. Many technologies against infections have been developed and undergone clinical trials. Such commercialized and successful technologies, such as coating medical devices, release antibiotics or nanoparticles to kill or retard their growth, thus, inhibiting the formation of biofilm and bacterial attachment. Intensive research must be performed in the direction of developing techniques to stop the formation of biofilms. More advanced mechanical testing methods for gentamicin-based coatings and composites should be developed. Comparatively, less literature and clinical studies are present for Mg-based implants [89].

A coating acts as a surface modification on the device, enables them to function as a biological carrier. The coating does not cause any biomechanical property change. Rather, it just benefits the device. The pertinent active substances can be delivered to the targeted site accordingly to the range of microorganisms present. In the present study, coating the devices with polymeric substances appropriately delivers such active substances at an emphatic concentration. Furthermore, many methods are available for the process of coating. Comparison between the different coating techniques is missing in the literature. However, it can be concluded that the dip-coating process is more effective with safety, durability and beautiful finishes. Additionally, a wide range of thickness, textures, and durometers might be made available to accommodate big volume orders requiring quick delivery, durability, and U.V. resistance. Furthermore, the strategies incorporating antibiotics, nanopatterning, and growth factors show potential for preventing bacterial adhesion by simultaneously intensifying healing and restoring the body tissues.

**Author Contributions:** A.T. and P.S. conceived the idea to write this review paper. A.T., P.S., B.V. and G.S. wrote the manuscript. B.V. provided useful insights into the manuscript. All authors have read and agreed to the published version of the manuscript.

**Funding:** The work received no external funding.

**Institutional Review Board Statement:** Not applicable.

**Informed Consent Statement:** Not applicable.

**Data Availability Statement:** The data is contained in the article itself.

**Acknowledgments:** The authors thank the Department of Metallurgical and Materials Engineering, Indian Institute of Technology, Kharagpur, India for their support.

**Conflicts of Interest:** The authors declare no conflict of interest.

## References

1. Office of the Surgeon General (US). Bone Health and Osteoporosis: A Report of the Surgeon General. Rockville (MD): Office of the Surgeon General (US); The Basics of Bone in Health and Disease. 2004; Volume 2. Available online: <https://www.ncbi.nlm.nih.gov/books/NBK45504/> (accessed on 3 August 2021).
2. Berry, S.D.; Miller, R.R. Falls: Epidemiology, pathophysiology, and relationship to fracture. *Curr. Osteoporos. Rep.* **2008**, *6*, 149–154. [[CrossRef](#)]
3. White, T.D.; Black, M.T.; Folkens, P.A. Chapter 1—Introduction. In *Human Osteology*, 3rd ed.; White, T.D., Black, M.T., Folkens, P.A., Eds.; Academic Press: San Diego, CA, USA, 2012; pp. 1–9. [[CrossRef](#)]
4. Gunn, C. *Bones and Joints-E-Book: A Guide for Students*, 6th ed.; Elsevier Health Sciences: Philadelphia, PA, USA, 2011.
5. Sahoo, N.; Anand, S.; Bhardwaj, J.; Sachdeva, V.; Sapru, B. Bone response to stainless steel and titanium bone plates: An experimental study on animals. *Med. J. Armed Forces India* **1994**, *50*, 10–14. [[CrossRef](#)]
6. Anderson, J.M.; Rodriguez, A.; Chang, D.T. Foreign body reaction to biomaterials. *Semin. Immunol.* **2008**, *20*, 86–100. [[CrossRef](#)]

7. Crincoli, V.; Cazzolla, A.P.; Di Comite, M.; Lo Muzio, L.; Ciavarella, D.; Dioguardi, M.; Bizzoca, M.E.; Palmieri, G.; Fontana, A.; Giustino, A.; et al. Evaluation of Vitamin D (25OHD), Bone Alkaline Phosphatase (BALP), Serum Calcium, Serum Phosphorus, Ionized Calcium in Patients with Mandibular Third Molar Impaction. An Observational Study. *Nutrients* **2021**, *13*, 1938. [[CrossRef](#)]
8. Berdal, A.; Bailleul-Forestier, I.B.I.; Davideau, J.-L.; LÉZot, F. CHAPTER 34 - Dento-alveolar Bone Complex and Vitamin D. In *Vitamin D*, 2nd ed.; Feldman, D., Ed.; Academic Press: Burlington, NJ, USA, 2005; pp. 599–607. [[CrossRef](#)]
9. Gallo, J.; Holinka, M.; Moucha, C.S. Antibacterial surface treatment for orthopaedic implants. *Int. J. Mol. Sci.* **2014**, *15*, 13849–13880. [[CrossRef](#)] [[PubMed](#)]
10. Saravanan, A. *Antibiotic Cement Impregnated Nailing in the Management of Infected Non Union of Femur and Tibia: A Prospective Study*; Kilpauk Medical College: Chennai, India, 2010.
11. Veerachamy, S.; Yarlagadda, T.; Manivasagam, G.; Yarlagadda, P.K. Bacterial adherence and biofilm formation on medical implants: A review. *Proc. Inst. Mech. Eng. Part H J. Eng. Med.* **2014**, *228*, 1083–1099. [[CrossRef](#)]
12. Horan, T.C.; Gaynes, R.P.; Martone, W.J.; Jarvis, W.R.; Grace Emori, T. CDC definitions of nosocomial surgical site infections, 1992: A modification of CDC definitions of surgical wound infections. *Am. J. Infect. Control* **1992**, *20*, 271–274. [[CrossRef](#)]
13. Lakdawala, M.; Hassan, P.; Kothwala, D.; Malik, G. Poly (D, L-Lactide)-Gentamicin composite coated orthopaedic metallic implant. *Int. J. Sci. Nat.* **2013**, *4*, 522–529.
14. Zaborowska, M.; Welch, K.; Brånemark, R.; Khalilpour, P.; Engqvist, H.; Thomsen, P.; Trobos, M. Bacteria-material surface interactions: Methodological development for the assessment of implant surface induced antibacterial effects. *J. Biomed. Mater. Res. Part B Appl. Biomater.* **2015**, *103*, 179–187. [[CrossRef](#)]
15. Krause, K.M.; Serio, A.W.; Kane, T.R.; Connolly, L.E. Aminoglycosides: An Overview. *Cold Spring Harb. Perspect. Med.* **2016**, *6*, a027029. [[CrossRef](#)] [[PubMed](#)]
16. Gonzalez, L.S., 3rd; Spencer, J.P. Aminoglycosides: A practical review. *Am. Fam. Physician* **1998**, *58*, 1811–1820.
17. Tamma, P.D.; Cosgrove, S.E.; Maragakis, L.L. Combination therapy for treatment of infections with gram-negative bacteria. *Clin. Microbiol. Rev.* **2012**, *25*, 450–470. [[CrossRef](#)]
18. Chen, C.; Chen, Y.; Wu, P.; Chen, B. Update on new medicinal applications of gentamicin: Evidence-based review. *J. Formos. Med Assoc. Taiwan Yi Zhi* **2014**, *113*, 72–82. [[CrossRef](#)]
19. Diana, G.; Margarida, P.; Ana Francisca, B. Osteomyelitis: An overview of antimicrobial therapy. *Braz. J. Pharm. Sci.* **2013**, *49*, 13–27.
20. Wen, Y.; Xu, J. Scientific Importance of Water-Processable PEDOT-PSS and Preparation, Challenge and New Application in Sensors of Its Film Electrode: A Review. *J. Polym. Sci. Part A Polym. Chem.* **2017**, *55*, 1121–1150. [[CrossRef](#)]
21. Birt, M.C.; Anderson, D.W.; Toby, E.B.; Wang, J. Osteomyelitis: Recent advances in pathophysiology and therapeutic strategies. *J. Orthop.* **2017**, *14*, 45–52. [[CrossRef](#)] [[PubMed](#)]
22. Andriole, V.T.; Nagel, D.A.; Southwick, W. Chronic staphylococcal osteomyelitis: An experimental model. *Yale J. Biol. Med.* **1974**, *47*, 33.
23. Orapiriyakul, W.; Young, P.S.; Damiati, L. Antibacterial surface modification of titanium implants in orthopaedics. *J. Tissue Eng.* **2018**, *9*, 2041731418789838. [[CrossRef](#)] [[PubMed](#)]
24. Dickinson, G.M.; Bisno, A.L. Infections associated with indwelling devices: Infections related to extravascular devices. *Antimicrob. Agents Chemother.* **1989**, *33*, 602. [[CrossRef](#)]
25. Ostermann, P.A.; Henry, S.L.; Seligson, D. Timing of wound closure in severe compound fractures. *Orthopedics* **1994**, *17*, 397–399. [[CrossRef](#)]
26. Lichter, J.A.; Van Vliet, K.J.; Rubner, M.F. Design of Antibacterial Surfaces and Interfaces: Polyelectrolyte Multilayers as a Multifunctional Platform. *Macromolecules* **2009**, *42*, 8573–8586. [[CrossRef](#)]
27. Upadhyayula, V.K.; Gadhamshetty, V. Appreciating the role of carbon nanotube composites in preventing biofouling and promoting biofilms on material surfaces in environmental engineering: A review. *Biotechnol. Adv.* **2010**, *28*, 802–816. [[CrossRef](#)]
28. Tuson, H.H.; Weibel, D.B. Bacteria-surface interactions. *Soft Matter* **2013**, *9*, 4368–4380. [[CrossRef](#)]
29. Hall-Stoodley, L.; Costerton, J.W.; Stoodley, P. Bacterial biofilms: From the natural environment to infectious diseases. *Nat. Rev. Microbiol.* **2004**, *2*, 95–108. [[CrossRef](#)] [[PubMed](#)]
30. Stoodley, P.; Sauer, K.; Davies, D.G.; Costerton, J.W. Biofilms as complex differentiated communities. *Annu. Rev. Microbiol.* **2002**, *56*, 187–209. [[CrossRef](#)] [[PubMed](#)]
31. Bernier, S.P.; Silo-Suh, L.; Woods, D.E.; Ohman, D.E.; Sokol, P.A. Comparative analysis of plant and animal models for characterization of *Burkholderia cepacia* virulence. *Infect. Immun.* **2003**, *71*, 5306–5313. [[CrossRef](#)] [[PubMed](#)]
32. Costerton, J.W.; Cheng, K.; Geesey, G.G.; Ladd, T.I.; Nickel, J.C.; Dasgupta, M.; Marrie, T.J. Bacterial biofilms in nature and disease. *Annu. Rev. Microbiol.* **1987**, *41*, 435–464. [[CrossRef](#)] [[PubMed](#)]
33. Costerton, J.W.; Stewart, P.S.; Greenberg, E.P. Bacterial biofilms: A common cause of persistent infections. *Science* **1999**, *284*, 1318–1322. [[CrossRef](#)] [[PubMed](#)]
34. Kunin, C.M. Blockage of urinary catheters: Role of microorganisms and constituents of the urine on formation of encrustations. *J. Clin. Epidemiol.* **1989**, *42*, 835–842. [[CrossRef](#)]
35. Reid, G. Biofilms in infectious disease and on medical devices. *Int. J. Antimicrob. Agents* **1999**, *11*, 223–226. [[CrossRef](#)]

36. Santos, A.L.S.d.; Galdino, A.C.M.; Mello, T.P.d.; Ramos, L.d.S.; Branquinha, M.H.; Bolognese, A.M.; Neto, J.C.; Roudbary, M. What are the advantages of living in a community? A microbial biofilm perspective! *Memórias Do Inst. Oswaldo Cruz* **2018**, *113*, 1–7. [[CrossRef](#)] [[PubMed](#)]
37. Habash, M.; Reid, G. Microbial biofilms: Their development and significance for medical device—related infections. *J. Clin. Pharmacol.* **1999**, *39*, 887–898. [[CrossRef](#)] [[PubMed](#)]
38. Del Pozo, J.; Patel, R. The challenge of treating biofilm-associated bacterial infections. *Clin. Pharmacol. Ther.* **2007**, *82*, 204–209. [[CrossRef](#)] [[PubMed](#)]
39. Alhede, M.; Er, Ö.; Eickhardt, S.; Kragh, K.; Alhede, M.; Christensen, L.D.; Poulsen, S.S.; Givskov, M.; Christensen, L.H.; Høiby, N. Bacterial biofilm formation and treatment in soft tissue fillers. *Pathog. Dis.* **2014**, *70*, 339–346. [[CrossRef](#)]
40. Garrett, T.R.; Bhakoo, M.; Zhang, Z. Bacterial adhesion and biofilms on surfaces. *Prog. Nat. Sci.* **2008**, *18*, 1049–1056. [[CrossRef](#)]
41. Cheng, G.; Li, G.; Xue, H.; Chen, S.; Bryers, J.D.; Jiang, S. Zwitterionic carboxybetaine polymer surfaces and their resistance to long-term biofilm formation. *Biomaterials* **2009**, *30*, 5234–5240. [[CrossRef](#)]
42. Roosjen, A.; van der Mei, H.C.; Busscher, H.J.; Norde, W. Microbial adhesion to poly (ethylene oxide) brushes: Influence of polymer chain length and temperature. *Langmuir* **2004**, *20*, 10949–10955. [[CrossRef](#)] [[PubMed](#)]
43. Schumacher, J.F.; Carman, M.L.; Estes, T.G.; Feinberg, A.W.; Wilson, L.H.; Callow, M.E.; Callow, J.A.; Finlay, J.A.; Brennan, A.B. Engineered antifouling microtopographies—effect of feature size, geometry, and roughness on settlement of zoospores of the green alga *Ulva*. *Biofouling* **2007**, *23*, 55–62. [[CrossRef](#)] [[PubMed](#)]
44. LING III, J.F.; GRAHAM, M.V.; CADY, N.C. Effect of topographically patterned poly (dimethylsiloxane) surfaces on pseudomonas aeruginosa adhesion and biofilm formation. *Nano Life* **2012**, *2*, 1242004. [[CrossRef](#)]
45. Salick, D.A.; Kretsinger, J.K.; Pochan, D.J.; Schneider, J.P. Inherent antibacterial activity of a peptide-based beta-hairpin hydrogel. *J. Am. Chem. Soc.* **2007**, *129*, 14793–14799. [[CrossRef](#)]
46. Laloyaux, X.; Fautré, E.; Blin, T.; Purohit, V.; Leprince, J.; Jouenne, T.; Jonas, A.M.; Glinel, K. Temperature-responsive polymer brushes switching from bactericidal to cell-repellent. *Adv. Mater. (Deerfield Beach Fla.)* **2010**, *22*, 5024–5028. [[CrossRef](#)]
47. Shukla, A.; Fleming, K.E.; Chuang, H.F.; Chau, T.M.; Loose, C.R.; Stephanopoulos, G.N.; Hammond, P.T. Controlling the release of peptide antimicrobial agents from surfaces. *Biomaterials* **2010**, *31*, 2348–2357. [[CrossRef](#)] [[PubMed](#)]
48. Kazemzadeh-Narbat, M.; Lai, B.F.; Ding, C.; Kizhakkedathu, J.N.; Hancock, R.E.; Wang, R. Multilayered coating on titanium for controlled release of antimicrobial peptides for the prevention of implant-associated infections. *Biomaterials* **2013**, *34*, 5969–5977. [[CrossRef](#)] [[PubMed](#)]
49. Wang, Y.; Jayan, G.; Patwardhan, D.; Phillips, K.S. Antimicrobial and anti-biofilm medical devices: Public health and regulatory science challenges. In *Antimicrobial Coatings and Modifications on Medical Devices*; Springer: New York, NY, USA, 2017; pp. 37–65.
50. Raschke, M.J.; Fuchs, T.; Stange, R.; Lucke, M.; Kandziora, F.; Wildemann, B.; Schmidmaier, G. Active Coating of Implants used in Orthopedic Surgery. In *Practice of Intramedullary Locked Nails: New Developments in Techniques and Applications*; Leung, K.-S., Taglang, G., Schnettler, R., Alt, V., Haarman, H.J.T.M., Seidel, H., Kempf, I., Eds.; Springer: Berlin/Heidelberg, Germany, 2006; pp. 283–296. [[CrossRef](#)]
51. Schmidmaier, G.; Wildemann, B.; Stemberger, A.; Haas, N.; Raschke, M. Biodegradable poly (D, L-lactide) coating of implants for continuous release of growth factors. *J. Biomed. Mater. Res. Off. J. Soc. Biomater. Jpn. Soc. Biomater. Aust. Soc. Biomater. Korean Soc. Biomater.* **2001**, *58*, 449–455. [[CrossRef](#)] [[PubMed](#)]
52. Qin, S.; Xu, K.; Nie, B.; Ji, F.; Zhang, H. Approaches based on passive and active antibacterial coating on titanium to achieve antibacterial activity. *J. Biomed. Mater. Res. Part A* **2018**, *106*, 2531–2539. [[CrossRef](#)] [[PubMed](#)]
53. Romanò, C.L.; Scarponi, S.; Gallazzi, E.; Romanò, D.; Drago, L. Antibacterial coating of implants in orthopaedics and trauma: A classification proposal in an evolving panorama. *J. Orthop. Surg. Res.* **2015**, *10*, 157. [[CrossRef](#)] [[PubMed](#)]
54. Romanò, C.L.; Tsuchiya, H.; Morelli, I.; Battaglia, A.G.; Drago, L. Antibacterial coating of implants: Are we missing something? *Bone Jt. Res.* **2019**, *8*, 199–206. [[CrossRef](#)] [[PubMed](#)]
55. Strobel, C.; Schmidmaier, G.; Wildemann, B. Changing the release kinetics of gentamicin from poly(D,L-lactide) implant coatings using only one polymer. *Int. J. Artif. Organs* **2011**, *34*, 304–316. [[CrossRef](#)]
56. Shi, Z.; Neoh, K.G.; Kang, E.T.; Wang, W. Antibacterial and mechanical properties of bone cement impregnated with chitosan nanoparticles. *Biomaterials* **2006**, *27*, 2440–2449. [[CrossRef](#)]
57. Staiger, M.P.; Pietak, A.M.; Huadmai, J.; Dias, G. Magnesium and its alloys as orthopedic biomaterials: A review. *Biomaterials* **2006**, *27*, 1728–1734. [[CrossRef](#)] [[PubMed](#)]
58. Wen, C.; Mabuchi, M.; Yamada, Y.; Shimojima, K.; Chino, Y.; Asahina, T. Processing of biocompatible porous Ti and Mg. *Scr. Mater.* **2001**, *45*, 1147–1153. [[CrossRef](#)]
59. Tencer, A.F.; Johnson, K.D. *Biomechanics in Orthopedic Trauma: Bone Fracture and Fixation*; Martin Dunitz London: London, UK, 1994; Volume 76, p. 1438.
60. Settle, F.A. *Handbook of Instrumental Techniques for Analytical Chemistry*; Prentice Hall PTR: Upper Saddle River, NJ, USA, 1997.
61. Chalmers, J.M.; Edwards, H.G.; Hargreaves, M.D. *Infrared and Raman Spectroscopy in Forensic Science*; John Wiley & Sons: New York, NY, USA, 2012.
62. McCreery, R.L. *Raman Spectroscopy for Chemical Analysis*; John Wiley & Sons: New York, NY, USA, 2005; Volume 225.
63. Witkowski, M.R. The use of Raman spectroscopy in the detection of counterfeit and adulterated pharmaceutical products. *Am. Pharm. Rev.* **2005**, *8*, 56.

64. McManamon, C.; Delaney, P.; Kavanagh, C.; Wang, J.J.; Rasappa, S.; Morris, M.A. Depth profiling of PLGA copolymer in a novel biomedical bilayer using confocal Raman spectroscopy. *Langmuir* **2013**, *29*, 5905–5910. [[CrossRef](#)]
65. Belu, A.; Mahoney, C.; Wormuth, K. Chemical imaging of drug eluting coatings: Combining surface analysis and confocal Raman microscopy. *J. Control. Release* **2008**, *126*, 111–121. [[CrossRef](#)]
66. Nast, S.; Fassbender, M.; Bormann, N.; Beck, S.; Montali, A.; Lucke, M.; Schmidmaier, G.; Wildemann, B. In vivo quantification of gentamicin released from an implant coating. *J. Biomater. Appl.* **2016**, *31*, 45–54. [[CrossRef](#)]
67. Li, Q.; He, G. Gelatin-enhanced porous titanium loaded with gentamicin sulphate and in vitro release behavior. *Mater. Des.* **2016**, *99*, 459–466. [[CrossRef](#)]
68. Pan, X.; Chen, S.; Li, D.; Rao, W.; Zheng, Y.; Yang, Z.; Li, L.; Guan, X.; Chen, Z. The synergistic antibacterial mechanism of gentamicin-loaded CaCO<sub>3</sub> nanoparticles. *Front. Chem.* **2018**, *5*, 130. [[CrossRef](#)] [[PubMed](#)]
69. Morawska-Chochół, A.; Domalik-Pyzik, P.; Chłopek, J.; Szaraniec, B.; Sterna, J.; Rzewuska, M.; Boguń, M.; Kucharski, R.; Mielczarek, P. Gentamicin release from biodegradable poly-L-lactide based composites for novel intramedullary nails. *Mater. Sci. Eng. C* **2014**, *45*, 15–20. [[CrossRef](#)] [[PubMed](#)]
70. Vester, H.; Wildemann, B.; Schmidmaier, G.; Stöckle, U.; Lucke, M. Gentamycin delivered from a PDLLA coating of metallic implants: In vivo and in vitro characterisation for local prophylaxis of implant-related osteomyelitis. *Injury* **2010**, *41*, 1053–1059. [[CrossRef](#)] [[PubMed](#)]
71. Boselli, E.; Allaouchiche, B. Diffusion in bone tissue of antibiotics. *Presse Med.* **1999**, *28*, 2265–2276.
72. Fraimow, H.S. Systemic antimicrobial therapy in osteomyelitis. *Semin. Plast. Surg.* **2009**, *23*, 90–99. [[CrossRef](#)]
73. Metsemakers, W.; Reul, M.; Nijs, S. The use of gentamicin-coated nails in complex open tibia fracture and revision cases: A retrospective analysis of a single centre case series and review of the literature. *Injury* **2015**, *46*, 2433–2437. [[CrossRef](#)]
74. Thonse, R.; Conway, J. Antibiotic cement-coated interlocking nail for the treatment of infected nonunions and segmental bone defects. *J. Orthop. Trauma* **2007**, *21*, 258–268. [[CrossRef](#)]
75. Morawska-Chochół, A.; Domalik-Pyzik, P.; Menaszek, E.; Sterna, J.; Bielecki, W.; Bonecka, J.; Boguń, M.; Chłopek, J. Biodegradable intramedullary nails reinforced with carbon and alginate fibers: In vitro and in vivo biocompatibility. *J. Appl. Biomater. Funct. Mater.* **2018**, *16*, 36–41. [[CrossRef](#)] [[PubMed](#)]
76. Raj, R.M.; Priya, P.; Raj, V. Gentamicin-loaded ceramic-biopolymer dual layer coatings on the Ti with improved bioactive and corrosion resistance properties for orthopedic applications. *J. Mech. Behav. Biomed. Mater.* **2018**, *82*, 299–309.
77. Saravanan, A.; Ganesh, R.R.; Ismail, N.D.M.; Anandan, H. Antibiotic Cement Impregnated Nailing in Management of Infected Non-union of Femur and Tibia. *Int. J. Sci. Study* **2017**, *5*, 187–191.
78. He, L.-J.; Hao, J.-C.; Dai, L.; Zeng, R.-C.; Li, S.-Q. Layer-by-layer assembly of gentamicin-based antibacterial multilayers on Ti alloy. *Mater. Lett.* **2020**, *261*, 127001. [[CrossRef](#)]
79. Bhatia, C.; Tiwari, A.; Sharma, S.; Thalanki, S.; Rai, A. Role of antibiotic cement coated nailing in infected nonunion of tibia. *Malays. Orthop. J.* **2017**, *11*, 6. [[PubMed](#)]
80. Vicenti, G.; Bizzoca, D.; Cotugno, D.; Carrozzo, M.; Riefoli, F.; Rifino, F.; Belviso, V.; Elia, R.; Solarino, G.; Moretti, B. The use of a gentamicin-coated titanium nail, combined with RIA system, in the management of non-unions of open tibial fractures: A single centre prospective study. *Injury* **2019**, *51*, S86–S91. [[CrossRef](#)]
81. Pinto, D.; Manjunatha, K.; Savur, A.D.; Ahmed, N.R.; Mallya, S.; Ramya, V. Comparative study of the efficacy of gentamicin-coated intramedullary interlocking nail versus regular intramedullary interlocking nail in Gustilo type I and II open tibia fractures. *Chin. J. Traumatol.* **2019**, *22*, 270–273. [[CrossRef](#)]
82. Moghaddam, A.; Graeser, V.; Westhauser, F.; Dapunt, U.; Kamradt, T.; Woerner, S.M.; Schmidmaier, G. Patients' safety: Is there a systemic release of gentamicin by gentamicin-coated tibia nails in clinical use? *Ther. Clin. Risk Manag.* **2016**, *12*, 1387.
83. Khodaei, M.; Valanezhad, A.; Watanabe, I. Controlled gentamicin-strontium release as a dual action bone agent: Combination of the porous titanium scaffold and biodegradable polymers. *J. Alloy. Compd.* **2017**, *720*, 22–28. [[CrossRef](#)]
84. Neut, D.; Dijkstra, R.J.; Thompson, J.I.; van der Mei, H.C.; Busscher, H.J. Antibacterial efficacy of a new gentamicin-coating for cementless prostheses compared to gentamicin-loaded bone cement. *J. Orthop. Res.* **2011**, *29*, 1654–1661. [[CrossRef](#)]
85. Raschke, M.; Vordemvenne, T.; Fuchs, T. Limb salvage or amputation? The use of a gentamicin coated nail in a severe, grade IIIc tibia fracture. *Eur. J. Trauma Emerg. Surg.* **2010**, *36*, 605–608. [[CrossRef](#)] [[PubMed](#)]
86. Lucke, M.; Schmidmaier, G.; Sadoni, S.; Wildemann, B.; Schiller, R.; Haas, N.; Raschke, M. Gentamicin coating of metallic implants reduces implant-related osteomyelitis in rats. *Bone* **2003**, *32*, 521–531. [[CrossRef](#)]
87. Gollwitzer, H.; Ibrahim, K.; Meyer, H.; Mittelmeier, W.; Busch, R.; Stemberger, A. Antibacterial poly(D,L-lactic acid) coating of medical implants using a biodegradable drug delivery technology. *J. Antimicrob. Chemother.* **2003**, *51*, 585–591. [[CrossRef](#)]
88. McMillan, D.J.; Lutton, C.; Rosenzweig, N.; Sriprakash, K.S.; Goss, B.; Stemberger, M.; Schuetz, M.A.; Steck, R. Prevention of Staphylococcus aureus biofilm formation on metallic surgical implants via controlled release of gentamicin. *J. Biomed. Sci. Eng.* **2011**, *4*, 535–542. [[CrossRef](#)]
89. Sharma, P.; Naushin, N.; Rohila, S.; Tiwari, A. Magnesium containing High Entropy Alloys. In *Magnesium Alloys Structure and Properties*; Tański, T.A., Ed.; IntechOpen: Rijeka, Croatia, 2021; pp. 1–26.